

<ul style="list-style-type: none"> <li>1121-1130</li> <li>1131-1140</li> <li>1141-1150</li> <li>1151-1160</li> <li>1161-1170</li> <li>1171-1180</li> <li>1181-1190</li> <li>1191-1200</li> <li>1201-1210</li> <li>1211-1220</li> <li>1221-1230</li> <li>1231-1240</li> <li>1241-1250</li> <li>1251-1260</li> <li>1261-1270</li> <li>1271-1280</li> <li>1281-1290</li> <li>1291-1300</li> <li>1301-1310</li> <li>1311-1320</li> <li>1321-1330</li> <li>1331-1340</li> <li>1341-1350</li> <li>1351-1360</li> <li>1361-1370</li> <li>1371-1380</li> <li>1381-1390</li> <li>1391-1400</li> <li>1401-1410</li> <li>1411-1420</li> <li>1421-1430</li> <li>1431-1440</li> <li>1441-1450</li> <li>1451-1460</li> <li>1461-1470</li> <li>1471-1480</li> <li>1481-1490</li> <li>1491-1500</li> <li>1501-1510</li> <li>1511-1520</li> <li>1521-1530</li> <li>1531-1540</li> <li>1541-1550</li> <li>1551-1560</li> <li>1561-1570</li> <li>1571-1580</li> <li>1581-1590</li> <li>1591-1600</li> <li>1601-1610</li> <li>1611-1620</li> <li>1621-1630</li> <li>1631-1640</li> <li>1641-1650</li> <li>1651-1660</li> <li>1661-1670</li> <li>1671-1680</li> <li>1681-1690</li> <li>1691-1700</li> <li>1701-1710</li> <li>1711-1720</li> <li>1721-1730</li> <li>1731-1740</li> <li>1741-1750</li> <li>1751-1760</li> <li>1761-1770</li> <li>1771-1780</li> <li>1781-1790</li> <li>1791-1800</li> <li>1801-1810</li> <li>1811-1820</li> <li>1821-1830</li> <li>1831-1840</li> <li>1841-1850</li> <li>1851-1860</li> <li>1861-1870</li> <li>1871-1880</li> <li>1881-1890</li> <li>1891-1900</li> <li>1901-1910</li> <li>1911-1920</li> <li>1921-1930</li> <li>1931-1940</li> <li>1941-1950</li> <li>1951-1960</li> <li>1961-1970</li> <li>1971-1980</li> <li>1981-1990</li> <li>1991-2000</li> </ul>	<ul style="list-style-type: none"> <li>1121-1130</li> <li>1131-1140</li> <li>1141-1150</li> <li>1151-1160</li> <li>1161-1170</li> <li>1171-1180</li> <li>1181-1190</li> <li>1191-1200</li> <li>1201-1210</li> <li>1211-1220</li> <li>1221-1230</li> <li>1231-1240</li> <li>1241-1250</li> <li>1251-1260</li> <li>1261-1270</li> <li>1271-1280</li> <li>1281-1290</li> <li>1291-1300</li> <li>1301-1310</li> <li>1311-1320</li> <li>1321-1330</li> <li>1331-1340</li> <li>1341-1350</li> <li>1351-1360</li> <li>1361-1370</li> <li>1371-1380</li> <li>1381-1390</li> <li>1391-1400</li> <li>1401-1410</li> <li>1411-1420</li> <li>1421-1430</li> <li>1431-1440</li> <li>1441-1450</li> <li>1451-1460</li> <li>1461-1470</li> <li>1471-1480</li> <li>1481-1490</li> <li>1491-1500</li> <li>1501-1510</li> <li>1511-1520</li> <li>1521-1530</li> <li>1531-1540</li> <li>1541-1550</li> <li>1551-1560</li> <li>1561-1570</li> <li>1571-1580</li> <li>1581-1590</li> <li>1591-1600</li> <li>1601-1610</li> <li>1611-1620</li> <li>1621-1630</li> <li>1631-1640</li> <li>1641-1650</li> <li>1651-1660</li> <li>1661-1670</li> <li>1671-1680</li> <li>1681-1690</li> <li>1691-1700</li> <li>1701-1710</li> <li>1711-1720</li> <li>1721-1730</li> <li>1731-1740</li> <li>1741-1750</li> <li>1751-1760</li> <li>1761-1770</li> <li>1771-1780</li> <li>1781-1790</li> <li>1791-1800</li> <li>1801-1810</li> <li>1811-1820</li> <li>1821-1830</li> <li>1831-1840</li> <li>1841-1850</li> <li>1851-1860</li> <li>1861-1870</li> <li>1871-1880</li> <li>1881-1890</li> <li>1891-1900</li> <li>1901-1910</li> <li>1911-1920</li> <li>1921-1930</li> <li>1931-1940</li> <li>1941-1950</li> <li>1951-1960</li> <li>1961-1970</li> <li>1971-1980</li> <li>1981-1990</li> <li>1991-2000</li> </ul>
--	--

# Cell Adhesion & Migration

ISSN: 1933-6918 (Print) 1933-6926 (Online) Journal homepage: <http://www.tandfonline.com/loi/kcam20>


## Transmigration characteristics of breast cancer and melanoma cells through the brain endothelium: role of Rac and PI3K

Judit Molnár, Csilla Fazakas, János Haskó, Orsolya Sipos, Krisztina Nagy, Ádám Nyúl-Tóth, Attila E. Farkas, Attila G. Végh, György Váró, Péter Galajda, István A. Krizbai & Imola Wilhelm

To cite this article: Judit Molnár, Csilla Fazakas, János Haskó, Orsolya Sipos, Krisztina Nagy, Ádám Nyúl-Tóth, Attila E. Farkas, Attila G. Végh, György Váró, Péter Galajda, István A. Krizbai & Imola Wilhelm (2015): Transmigration characteristics of breast cancer and melanoma cells through the brain endothelium: role of Rac and PI3K, *Cell Adhesion & Migration*, DOI: [10.1080/19336918.2015.1122156](https://doi.org/10.1080/19336918.2015.1122156)

To link to this article: <http://dx.doi.org/10.1080/19336918.2015.1122156>

 View supplementary material 

 Accepted author version posted online: 08 Dec 2015.

 Submit your article to this journal 

 Article views: 1

 View related articles 

 View Crossmark data 

Full Terms & Conditions of access and use can be found at <http://www.tandfonline.com/action/journalInformation?journalCode=kcam20>

Role of Rac and PI3K in the interaction of tumor cells with the BBB

**Transmigration characteristics of breast cancer and melanoma cells through the brain endothelium: role of Rac and PI3K**

Judit Molnár<sup>1</sup>, Csilla Fazakas<sup>1</sup>, János Haskó<sup>1</sup>, Orsolya Sipos<sup>1</sup>, Krisztina Nagy<sup>1</sup>, Ádám Nyúl-Tóth<sup>1</sup>, Attila E. Farkas<sup>1</sup>, Attila G. Végh<sup>1</sup>, György Váró<sup>1</sup>, Péter Galajda<sup>1</sup>, István A. Krizbai<sup>1,2</sup>, Imola Wilhelm<sup>1</sup>

<sup>1</sup>Institute of Biophysics, Biological Research Centre, Hungarian Academy of Sciences, Szeged, Hungary

<sup>2</sup>Institute of Life Sciences, Vasile Goldis Western University of Arad, Arad, Romania

**Corresponding author:**

Imola Wilhelm, Institute of Biophysics, Biological Research Centre, Hungarian Academy of Sciences, Temesvári krt. 62, 6726, Szeged, Hungary, Tel. +36-62-599601, Fax. +36-62-433133, E-mail: wilhelm.imola@brc.mta.hu

**ABSTRACT**

Brain metastases are common and devastating complications of both breast cancer and melanoma. Although mammary carcinoma brain metastases are more frequent than those originating from melanoma, this latter has the highest tropism to the brain. Using static and dynamic in vitro approaches, here we show that melanoma cells have increased adhesion to the brain endothelium in comparison to breast cancer cells. Moreover, melanoma cells can

transmigrate more rapidly and in a higher number through brain endothelial monolayers than breast cancer cells. In addition, melanoma cells have increased ability to impair tight junctions of cerebral endothelial cells. We also show that inhibition of Rac or PI3K impedes adhesion of breast cancer cells and melanoma cells to the brain endothelium. In addition, inhibition of Rac or PI3K inhibits the late phase of transmigration of breast cancer cells and the early phase of transmigration of melanoma cells. On the other hand, the Rac inhibitor EHT1864 impairs the junctional integrity of the brain endothelium, while the PI3K inhibitor LY294002 has no damaging effect on interendothelial junctions. We suggest that targeting the PI3K/Akt pathway may represent a novel opportunity in preventing the formation of brain metastases of melanoma and breast cancer.

**Keywords:** breast cancer, melanoma, brain metastasis, blood-brain barrier, cerebral endothelial cell, adhesion, transmigration, Rac, PI3K

**List of abbreviations:**

BBB	blood-brain barrier
CEC	cerebral endothelial cell
CNS	central nervous system
D3 (hCMEC/D3)	human cerebral microvascular endothelial cells, clone D3
GEF	guanine nucleotide exchange factor
PI3K	phosphoinositide 3-kinase

RBEC                      rat brain endothelial cell

ROCK                     Rho-kinase

Accepted Manuscript

## INTRODUCTION

Brain metastases – which are usually late, but devastating complications of cancer – most frequently originate from lung cancer, breast cancer and melanoma. Tumor cells successfully infiltrating the brain parenchyma overcome several obstacles, including survival in the circulation, <sup>1</sup> extravasation through brain capillaries (reviewed in: <sup>2</sup>) and resisting deleterious signals of the reactive brain stroma. <sup>3</sup> However, cancer cells able to migrate into and to survive in the brain will benefit of a supportive and protective microenvironment, including the dense vasculature with the opportunity of vessel co-option <sup>4</sup> and chemoprotection mediated by astrocytes and endothelial cells. <sup>5</sup> As a consequence, brain metastases have a poor prognosis. Therefore, inhibiting extravasation of metastatic cells into the brain would be of great clinical benefit.

Diapedesis of metastatic cells through the capillaries of the brain implies adhesion of tumor cells to the luminal surface of cerebral endothelial cells (CECs), followed by a recently described, not yet fully characterized step called incorporation into the monolayer, <sup>6</sup> and finally the transmigration step itself. CECs are interconnected by a continuous layer of tight junctions and form the blood-brain barrier (BBB). The BBB restricts the free movement of solutes between the blood and the central nervous system, and represents an impediment for cellular elements (leukocytes and metastatic cells) to reach the brain parenchyma (reviewed in: <sup>7</sup>). We have previously shown that melanoma cells are able to disrupt the tight junctions of CECs making possible their transmigration through the brain endothelium. <sup>8</sup> It is not understood however,

whether breast cancer cells are able to disrupt the tight junctions or migrate preferentially transcellularly. In fact, transcellular migration of tumor cells has only been described in case of breast cancer cells during intravasation into an in vitro vascular network<sup>9</sup> and migration through umbilical cord endothelial cells.<sup>10</sup> However, to our knowledge, no data on the transmigration pathway of breast cancer cells through BBB endothelial cells exist.

Our previous results indicated that during transmigration through the brain endothelium, melanoma cells favor the mesenchymal type of cell movement.<sup>11</sup> This is characterized by an elongated morphology, increased proteolytic activity and is dependent on Rac activity.<sup>12</sup> On the other hand, the amoeboid type of tumor cell migration is characterized by rounded morphology and extensive RhoA signaling. Tumor cells can switch between these two movement types depending on the environment they move in.<sup>13</sup> By inhibiting Rho/ROCK signaling, and therefore triggering the mesenchymal phenotype, a significant increase in the number of melanoma cells migrating through CECs could be induced.<sup>11</sup> Here we aimed to compare melanoma and breast cancer cells in respect of mesenchymal vs. amoeboid migration through the brain endothelium. The question whether tumor cells prefer Rho/ROCK or Rac-dependent transendothelial migration is of clinical importance, since inhibitors of both Rho/ROCK (e.g. fasudil) and Rac pathways<sup>14</sup> are emerging as potential therapeutic agents.

The Rac pathway has been shown to be regulated by phosphoinositide 3-kinase (PI3K) in breast cancer cells.<sup>15</sup> Moreover, the PI3K/Akt/mTOR pathway is probably the most important in respect of anti-cancer treatment targets.<sup>16</sup> It has been shown that dysregulation of the PI3K signaling pathway is associated with the development of one-third of human cancers, including

breast cancers<sup>17</sup> and melanomas.<sup>18</sup> Aberrant activation of the PI3K pathway promotes carcinogenesis, tumor angiogenesis and resistance to therapies,<sup>19</sup> and plays a role in cell motility as well.<sup>20</sup>

Therefore, the first aim of our study was to compare the adhesion and transmigration properties of melanoma and breast cancer cells. The second aim was to understand the role of Rac signaling and of amoeboid vs. mesenchymal phenotype in the transmigration of breast cancer cells through the BBB. The third aim was to investigate whether PI3K inhibition has an impact on the transmigration of tumor cells through the cerebral endothelium during brain metastasis formation.

## **RESULTS**

### **Adhesion and transmigration properties of melanoma and breast cancer cells in vitro**

Since melanoma cells have higher propensity to metastasize to the brain than breast cancer cells, we aimed to understand whether there is any difference in the interaction of melanoma cells or breast cancer cells with the brain endothelium.

We first aimed to compare the adhesion properties of melanoma and breast cancer cells to the brain endothelium. 90 min after plating the tumor cells upon brain endothelial cells, significantly more melanoma cells than breast cancer cells were able to attach to the endothelium (Table 1).

Therefore, we wanted to test whether the increased adhesion of melanoma cells in comparison to breast cancer cells results in an increased transmigration as well.

For studying the transmigration properties of melanoma and breast cancer cells in static conditions, we used a novel approach based on a time-lapse video setup described in the Materials and methods section. This innovative assay developed in our laboratory makes possible to follow the fate of each individual cell in time (adhesion, migration, division, etc.). This approach eliminates the drawbacks of assays using filter inserts, where cells migrating through the endothelial monolayer but not moving through the pores of the filter cannot be considered. Moreover, several cell types (including D3 cells) cannot be properly grown on large pore-size filters due to the formation of a double monolayer on both sides of the membrane.

Comparing the transmigration properties of melanoma and breast cancer cells using the static transmigration assay, we observed that fewer breast cancer cells than melanoma cells were able to migrate through the brain endothelium (Table 2). The difference was significant: 27-28% of plated melanoma cells completed the transmigration process, while only 16% of breast cancer cells migrated through.

To confirm our results in physiologically more relevant conditions, we constructed a dynamic transmigration model. Brain endothelial cells were cultured in a microfluidic device (Fig. 1A; described in details in the Material and methods section) until confluence (Suppl. video 1). After reaching confluence, a slow, physiologically relevant flow of the culture medium was initiated (300  $\mu\text{l/h}$ , 1-2  $\text{dyn/cm}^2$ ) for 24 h. Shear stress induced elongation of endothelial cells (Suppl. Fig. 1). After injection of MDA-MB-231 or A2058 cells, the flow was re-started with a rate of 100



$\mu\text{l/h}$ , phase-contrast images were taken and time-lapse videos were constructed to analyze the movements of the tumor cells (Fig. 1B, Suppl. videos 2 and 3).

In these conditions approximately 50% of breast cancer cells and 42.5% of melanoma cells showed no attachment and were washed away by the flow of the culture medium in early stages of the experiment (Fig. 1B: white circles, Table 3: no attachment). The percentage of tumor cells not washed away from the optical fields studied, but not able to transmigrate in 6 h, was significantly more in case of breast cancer cells than in case of melanoma cells (15% vs. 4.5%, respectively) (Fig. 1B: black circles, Table 3: no transmigration). Taken together, 53% of melanoma and 35% of breast cancer cells transmigrated through the brain endothelial monolayer in these conditions. The difference in the transmigration between the two cell types was the most pronounced in early time points: 23.5% of the total number of melanoma cells migrated through the brain endothelium in the first 20 min, while the percentage of breast cancer cells transmigrating in this time frame was only 3% (Fig. 1B: white arrows, Table 3: transmigr. in 20 min). Melanoma cells tended to attach and transmigrate in small groups (Fig. 1B: grey dotted star), as we have previously observed in static conditions.<sup>8</sup> After transmigration, several melanoma cells continued to move beneath and between endothelial cells (as previously seen in static conditions<sup>8</sup>), sometimes rounding up and flattening again (Fig. 1B: cells 1 and 2). A few divisions were also observed (Fig. 1B: black boxes) and the daughter cells usually transmigrated rapidly after division (Fig. 1B: cell 3).

Taken together, these results show that melanoma cells are able to adhere to and migrate through the brain endothelium more effectively than breast cancer cells. This might be partly responsible for the higher propensity of melanoma cells to metastasize to the brain.

### **Differences in the effects of melanoma cells and breast cancer cells on the tight junctions of brain endothelial cells**

We have previously observed that during transmigration melanoma cells are able to disrupt the tight junctions of cerebral endothelial cells and use (at least partly) the paracellular way of migration.<sup>8</sup> We were interested to understand whether breast cancer cells are also able to impair the junctional integrity of the cerebral endothelium. Therefore, we performed claudin-5 immunostaining on primary rat brain endothelial cell (RBEC) monolayers challenged either with MDA-MB-231 breast cancer or with A2058 melanoma cells. As shown on Fig. 2, melanoma cells could breach the junctions of RBECs as indicated by focal loss of claudin-5 staining. This was not observed in case of breast cancer cells.

These data suggest that differences in the transendothelial migration of mammary carcinoma and melanoma cells might be partly due to differences in their ability to impair interendothelial junctions.

## **Inhibition of Rac or PI3K hampers the adhesion of breast cancer cells and melanoma cells to the brain endothelium**

We have previously shown that inhibition of the Rho/ROCK pathway facilitates the adhesion of melanoma cells, and this effect is reversed by the Rac inhibitor EHT1864.<sup>11</sup> We now aimed to understand whether the same mechanism applies for breast cancer cells during adhesion to cerebral endothelial cells. In contrast to melanoma cells, ROCK inhibitors (10  $\mu$ M Y27632 or 10  $\mu$ M fasudil) were not able to increase the number of breast cancer cells adherent to the brain endothelium (Fig. 3A). On the other hand, the Rac inhibitor EHT1864 (20  $\mu$ M) hampered the adhesion of both MDA-MB-231 and MCF-7 breast cancer cells (Fig. 3A and B). As expected, mainly the number of elongated adherent cells was decreased, which have a mesenchymal phenotype. When both ROCK and Rac inhibitors were applied, a similar reduction in the adhesion of tumor cells was seen as with the Rac inhibitor alone (Fig. 3A). In addition, the PI3K inhibitor LY294002 in a concentration of 25  $\mu$ M significantly reduced the number of breast cancer and melanoma cells attaching to the brain endothelium. The reduction was approximately 40% compared to control in case of both breast cancer and melanoma cells, and mainly affected tumor cells with elongated (flattened, mesenchymal) phenotype (Fig. 3A-C). In case of A375 melanoma cells, which presented a rounded morphology during adhesion, LY294002 could also significantly reduce the number of adherent cells (Fig. 3D).

Interestingly, when measuring the adhesion forces using atomic force microscopy between MDA-MB-231 breast cancer and hCMEC/D3 brain endothelial cells, or A2058 melanoma and

hCMEC/D3 brain endothelial cells, respectively, we could not observe any decrease in response to EHT1864 or LY294002 (Suppl. Fig. 2).

### **Inhibition of Rac or PI3K impedes the transmigration of breast cancer cells and melanoma cells through the brain endothelium in static conditions**

Since inhibition of Rac or PI3K decreased the adhesion of both melanoma and breast cancer cells, we tested the effect of Rac or PI3K inhibitors on the transmigration of melanoma and breast cancer cells through brain endothelial monolayers as well (Fig. 4). In this assay we used two invasive melanoma cell lines (A2058 and A375) and the MDA-MB-231 breast cancer cell line, which is more invasive than the MCF-7 cell line. Inhibition of Rac with EHT1864 significantly reduced the transmigration of both tumor cell types to approximately 20% in case of breast cancer cells (Fig. 4A) and to 15% in case of melanoma cells (Fig. 4C). LY294002 had similar effects: the transmigration percentage was approximately 30% and 40%, respectively, compared to control (Fig. 4B, D, E).

### **Inhibition of Rac or PI3K inhibits the late phase of transmigration of breast cancer cells and the early phase of transmigration of melanoma cells through the brain endothelium in dynamic conditions**

Using our dynamic model, we explored which step of transmigration of breast cancer or melanoma cells was inhibited by EHT1864 or LY294002. As previously discussed (Table 3),

only 8% of total transmigrating breast cancer cells completed transmigration in the first 20 min (2.8% of 35%), while this was significantly higher in case of melanoma cells (44.34%, i.e. 23.5% of 53%). This suggests that melanoma cells can transmigrate more rapidly through the brain endothelium than breast cancer cells (Fig. 5). Nevertheless, EHT1864 and LY294002 inhibited the rapid transmigration of melanoma cells. However, in case of breast cancer cells the number of cells transmigrating after 20 min was reduced by inhibitors of Rac and PI3K (Fig. 5).

Taken together, our results indicate that inhibition of Rac or PI3K impairs the ability of both breast cancer and melanoma cells to adhere to and to migrate through the brain endothelium. Differences exist however, between the velocities of the transmigration of the two tumor cell types.

### **Effects of Rac and PI3K inhibitors on the viability, proliferation and migration of tumor cells and brain endothelial cells**

We wanted to exclude that the inhibitory effect of EHT1864 and LY294002 on the adhesion and transmigration of breast cancer and melanoma cells was due to toxicity on tumor cells. Using the EZ4U assay no toxic effect of either EHT1864 or LY294002 on A2058, MDA-MB-231 and MCF-7 cells was observed (not shown). Moreover, the EZ4U assay did not show any toxicity of EHT1864 or LY294002 on D3 brain endothelial cells. In addition, as assessed during the time-lapse video experiments, the number of dividing cells was approximately 2.5% in case of MDA-MB-231 cells and 1% in case of A2058 cells. Therefore, the observed changes in the adhesion and transmigration are unlikely to be the result of an anti-proliferative effect of EHT1864 or

LY294002. Moreover, the wound healing assay indicated no change in the migratory properties of melanoma or breast cancer cells in response to EHT1864 or LY294002 (not shown).

### **The Rac inhibitor EHT1864 impairs the junctional integrity of the brain endothelium**

We observed that EHT1864 induced a decrease in the impedance of D3 cells, as reflected by the cell index on Fig. 6A. After an initial drop induced by the medium change, the impedance of control and LY294002-treated D3 cells recovered rapidly. However, in case of EHT1864-treated cells the recovery was not complete, and after 5 h a significant drop in the impedance was seen. The cell impedance reflects changes in the cell number, viability and tightness of the junctions. Since no change in the viability of D3 cells was observed using the EZ4U assay, we next investigated the possible damaging effect of the Rac inhibitor on the tight junctions. We observed a significant down-regulation of claudin-5 protein in D3 cells in response to EHT1864 (Fig. 6B). LY294002 did not significantly affect the amount of claudin-5 protein in D3 cells.

## **DISCUSSION**

Brain metastases are devastating complications of lung cancer, breast cancer, melanoma and other malignancies. Among all solid tumors, melanoma has the highest affinity to the central nervous system. This has been explained by the specific brain environment which supports the growth of cells of ectodermal origin.<sup>21, 22</sup> However, besides soluble and cellular elements of the

central nervous system, other factors might also contribute to the neurotropism of melanoma cells.

One of the most important steps in the process of brain metastasis formation is the diapedesis of metastatic cells through the barriers of the CNS, mainly the BBB-forming microvascular endothelium. The role of the BBB in the formation of cerebral metastases is largely unexplored and probably very complex. Being the tightest endothelial barrier in the organism, it hinders the transmigration of tumor cells into the brain. On the other hand, unique brain endothelial properties might differentially affect the diapedesis of different cancer cell types.<sup>2</sup>

Our results indicate that melanoma cells have increased adhesion to the brain endothelium than breast cancer cells. In order to exclude the possibility that this is due to differences in the invasive and metastatic capacities between the melanoma and breast cancer cell lines used, we used two different breast cancer cell lines: the less invasive MCF-7 and the highly migratory and metastatic MDA-MB-231.<sup>14</sup> We also used two different melanoma cell lines, A2058 and A375, both invasive BRAF V600E mutants, having similar propensity to metastasize to different organs,<sup>23</sup> A2058 being vemurafenib resistant, while A375 vemurafenib sensitive.<sup>24</sup> The difference between the adhesive properties of melanoma cells and either of the breast cancer cell lines was significant. Moreover, such a difference was not observed when other endothelial cell types (HUVECs, dermal microvascular cells, lymphatic endothelial cells) were used: melanoma cells had similar adhesion properties to non-cerebral endothelial cells as breast cancer cells.<sup>25</sup> On the other hand, incorporation of A375 into HUVECs was shown to be faster than that of MDA-MB-321.<sup>6</sup> We have also observed a significant difference in the number of transmigrating

melanoma and breast cancer cells. The number of cells not able to migrate through the brain endothelium was much higher in case of breast cancer cells than in case of melanoma cells. Moreover, invasive melanoma cells tended to complete the transmigration process much more rapidly than invasive breast cancer cells. These data suggest that tumor cells with higher affinity to the brain can more easily overcome the BBB; however, further studies are needed to support this hypothesis.

Differences between the ability of the two tumor cell types to migrate through the brain endothelium might be partly due to their different ability to impair the tight junctions. Our data indicate that melanoma cells are more effective in breaking down the paracellular barrier than breast cancer cells. Breast cancer cells were previously shown to be able to use not only the paracellular pathway (through interendothelial junctions), but also the transcellular pathway (through the endothelial cell body) during migration through non-cerebral endothelia.<sup>9, 10</sup> Our results suggest that breast cancer cells might be more effective in the transcellular type of migration than melanoma cells, these latter having increased ability to impair the tight junctions than mammary carcinoma cells. Further analyses will clarify this possible difference between the two tumor cell types.

We have also assessed the role of two signaling molecules (Rac and PI3K) in the transmigration of melanoma and breast cancer cells through the BBB. In a recent study we showed that melanoma cells prefer the Rac-dependent mesenchymal type of cell movement to the Rho/ROCK-dependent amoeboid one during transmigration through the BBB.<sup>11</sup> Here we show that inhibition of Rac not only impedes the adhesion and transmigration of melanoma cells, but



of breast cancer cells as well. According to our previous results, ROCK inhibition induced an increase in the adhesion force between melanoma and brain endothelial cells. We hypothesized that mesenchymal cell flattening was partly responsible for this phenomenon.<sup>11</sup> We suppose that induction of the amoeboid phenotype using the Rac inhibitor does not have such a significant impact on the shape of tumor cells detached from the surface. Therefore, the area of contact between tumor cells and endothelial cells does not significantly differ between control and Rac-inhibited tumor cells, resulting in similar adhesion forces in the presence or absence of EHT1864, as measured by AFM.

Interestingly, the ROCK inhibitors Y27632 or fasudil – which significantly facilitated the adhesion of melanoma cells<sup>11</sup> – did not affect the adhesive properties of breast cancer cells. However, the effect of Rac inhibition was similar in case of both melanoma and breast cancer cells: a significant decrease in the number of tumor cells attaching to and transmigrating through cerebral endothelial cells was observed. This supports the idea that inhibition of the mesenchymal movement of tumor cells might be beneficial in reducing the diapedesis of different metastatic cells through the BBB. Unfortunately, Rac inhibitors – in contrast to ROCK inhibitors, which prevent the disruption of the tight junctions of CECs – might impair the integrity of the BBB.

Besides Rac, we tested the role of the PI3K/Akt/PTEN pathway, which is a key regulator of tumorigenesis and metastasis formation. BRAF-mutant melanoma cells have been shown to have higher levels of pAkt-Ser473, pAkt-Thr308 and decreased expression of PTEN.<sup>26</sup> The A2058 cell line used in our experiments is a V600E BRAF mutant expressing high amounts of

phosphorylated Akt and low levels of PTEN.<sup>27</sup> It has been shown that inhibition of PI3K results in a reduction of melanoma cell transmigration through HUVECs.<sup>28</sup> Since brain metastases of melanoma have been shown to have significantly higher pAkt and lower PTEN levels than extracerebral metastases,<sup>26, 29</sup> we aimed to test whether inhibition of this pathway impedes the transmigration of melanoma cells through CECs. We observed a marked inhibition of melanoma cells able to attach to and to migrate through the brain endothelium in response to PI3K inhibition. This is in contrast with small cell lung cancer cells, which were not affected by PI3K inhibition in their transmigration through brain microvascular endothelial cells.<sup>30</sup> It has been previously shown that inhibition of Rac or PI3K, but of ROCK also reduces the pulmonary microvascular endothelial cell-induced invasiveness of MDA-MB-231 with high  $\alpha_5\beta_1$  integrin expression.<sup>31</sup> According to our results, breast cancer cell transendothelial migration could be partly blocked using the PI3K inhibitor LY294002 – similarly to melanoma cells.

The morphology of PI3K-inhibited tumor cells was similar to that of Rac-inhibited cells, i.e. we could see a reduction in the number of elongated, flattened cells. This suggests that PI3K inhibition – similar to Rac inhibition – induces an amoeboid-like phenotype in both melanoma and breast cancer cells. This is not surprising because PI3K has been shown to regulate Rac through P-Rex1 in breast cancer cells<sup>15</sup> and several PI3K lipid products have been shown to interact with different RacGEFs.<sup>32</sup>

In contrast to EHT1864, the PI3K inhibitor LY294002 did not affect the integrity of the BBB. Moreover, many PI3K inhibiting agents are in different phases of clinical trials for the treatment of different cancer types.<sup>33</sup> Based on our results, PI3K inhibitors might turn out to have clinical

benefits not only in the treatment of primary tumors, but also in preventing brain metastasis formation of breast cancer and melanoma cells.

In conclusion, we have shown that invasive melanoma cells have an increased capacity to attach to, to migrate through and to impair the tight junctions of the brain endothelium than breast cancer cells. In addition, inhibition of Rac or PI3K decreases the number of both melanoma and breast cancer cells able to transmigrate through cerebral endothelial cells; however, Rac inhibition (but not PI3K inhibition) impairs the junctional integrity of the blood-brain barrier. Since inhibitors of the PI3K/Akt pathways are emerging as candidates for anti-cancer therapy, the mechanism described here might be of clinical relevance.

## **MATERIALS AND METHODS**

### **Cell culture and treatments**

MDA-MB-231 and MCF-7 human breast cancer cells were kept in DMEM medium (Sigma) supplemented with 5% FBS (Lonza). A2058 human melanoma cells (obtained from the European Collection of Cell Cultures) were maintained in EMEM (Sigma) supplemented with 5% FBS (Sigma). A375 human melanoma cells were kept in DMEM medium (Sigma) supplemented with 10% FBS (Lonza). The hCMEC/D3 human microvascular cerebral endothelial cells (abbreviated as D3) were grown on rat tail collagen-coated dishes in EBM-2 medium (Lonza) supplemented with EGM-2 Bullet Kit (Lonza) and 2.5% FBS (Sigma). Rat

brain endothelial cells (RBECs) used for immunofluorescence experiments were isolated and cultured as described previously.<sup>34</sup>

ROCK inhibitors (Y27632, Tocris and fasudil, Santa Cruz) were used in a final concentration of 10  $\mu$ M. EHT1864 (Tocris), an inhibitor of Rac family GTPases, was applied in a 20  $\mu$ M concentration. LY294002 (Cell Signaling Technology) – a reversible and highly selective inhibitor of phosphatidylinositol 3 kinase (PI3K) – was used in a concentration of 25  $\mu$ M.

### **Adhesion experiments**

Brain endothelial cells (D3) were grown until confluence in 24-well plates. Tumor cells (MDA-MB-231, MCF-7 or A2058 cells) were fluorescently labeled using Oregon Green 488 carboxylic acid diacetate succinimidyl ester or Cell Tracker red (Life Technologies) using the protocol supplied by the manufacturer.  $5 \times 10^4$  tumor cells/well were plated onto the endothelial monolayer in serum-free medium and incubated for 90 min. Non-attached cells were washed and the remaining cells were fixed using ethanol/acetic acid (95/5) at  $-20^{\circ}\text{C}$  for 5 min. Tumor cells adhered to endothelial cells were photographed and counted using the Image-Pro Plus software (Media Cybernetics).

## **Adhesion force measurements**

Single cell force spectroscopy measurement of adhesion forces between tumor cells and endothelial cells using atomic force microscopy (AFM) was performed as previously described in details.<sup>11</sup>

## **Static transmigration experiments using time-lapse video imaging**

Human cerebral endothelial cells (D3) were cultured until confluence in 12-well plates.  $2 \times 10^4$ /well tumor cells were plated onto the endothelial monolayer in Leibovitz's L-15 medium (Sigma). Cells were monitored for 6 h using an Andor NEO sCMOS camera connected to a Nikon Eclipse Ti-E inverted microscope, equipped with a home built incubator set to 37°C. Phase-contrast images were made every 5 min from 5 optical fields/well and time-lapse videos were constructed. The movement of each tumor cell was evaluated and transmigrated cells were counted.

## **Dynamic transmigration experiments using microfluidics**

### *Design and fabrication of microdevices*

To investigate the transmigration of tumor cells under low shear stress conditions we designed and constructed a biocompatible artificial capillary network. The schematic representation of the microfluidic setup is shown in Fig. 1A. The microfluidic capillary device was fabricated from

poly-dimethylsiloxane (PDMS, Sylgard 184, Dow Corning Corp.) using standard photolithography and soft lithography techniques.<sup>35</sup> Imprints of the microdevices were built by creating 100  $\mu\text{m}$  high SU8-2050 negative photoresist (MicroChem Corp.) layers on silicon wafers. The photoresist layers were exposed to UV light through a chromium mask (JD Photo-Tools Ltd.), using a flood exposure source with mask aligner (500W Hg lamp, i-line, model 97435, Newport Corp. & Digital Exposure Controller model 68945, Newport Corp.). In order to prevent the attachment of PDMS to the SU8 molds, the molds were treated with tridecafluoro-1,1,2,2-tetrahydrooctyl-trichlorosilane (Gelest Inc.) under vacuum overnight. Positive replicas were fabricated by PDMS molding. The PDMS replicas were cured, inlet holes and bubble traps were punched and the devices were bound to PDMS-covered microscope glass slides using oxygen plasma treatment.

#### *Cell seeding and microfluidic cell culture*

Prior to seeding of brain endothelial cells, the inner surface of the channels was coated with rat tail collagen.  $10^6$  D3 cells were collected in 100  $\mu\text{l}$  Leibovitz's L-15 media completed with 2.5% FBS (Sigma), growth factor mix (Lonza), hydrocortisone and gentamicin-amphotericin-B and injected into the microchannels. The microfluidic devices were placed in a home built incubator installed on a microscope stage set to 37°C. Cells were kept in "static conditions" for 24-36 h to reach a confluent layer. During this static state the D3 medium was refreshed every 8 h. When the confluent endothelial layer fully developed, a continuous flow at 300  $\mu\text{l}/\text{h}$  rate was started and maintained for 24 h to mimic the blood circulation.

During the transmigration experiments  $3 \times 10^5$  tumor cells were collected in 100  $\mu\text{l}$  media and injected manually (with syringe). After the injection, a continuous flow with 100  $\mu\text{l}/\text{h}$  rate was established and maintained for 6 h. Considering the physical parameters of the device (channel height of  $\sim 100 \mu\text{m}$ , channel width of  $\sim 240\text{-}480 \mu\text{m}$ ) and the used fluid flow rates (100-300  $\mu\text{l}/\text{h}$ ), we can estimate the shear stress (based on <sup>36</sup>) acting on the endothelial cells in the microchannels. The applied fluid flow generated a low stress regime in our device, in which the shear stress was around  $\sim 0.3\text{-}2 \text{ dyn}/\text{cm}^2$ .

### *Microscopy*

Phase contrast microscopy images were taken during the cell culturing and the transmigration experiments, using an Andor NEO sCMOS camera and a Nikon Eclipse Ti-E microscope (Nikon Inc.), equipped with a 20 $\times$  Plan Fluor phase contrast objectives and a Proscan II motorized microscope stage (Prior Scientific Ltd.). We used the Nikon NIS Elements AR software (Nikon Inc.) to control the microscope setup during the recordings. Microscopy images were taken every 30 min during the endothelial cell attachment phase and every 5 min during the transmigration experiments (representative images are shown on Fig. 1B).

### *Image analysis*

We followed each individual tumor cell in 6 fields/microchannel. Total number of cells counted was considered 100% in case of each microchannel. Cells were classified in one of the following groups: “no attachment” (cells washed away by the flow of the culture medium in early stages of the experiment), “no transmigration” (cells remaining attached to the endothelial layer but not able to transmigrate in 6 h), “transmigr. in 20 min” or “transmigr. in  $>20$  min”. Comparison was

performed among the four groups in case of each cell type and each treatment, among control and EHT1864- or LY294002-treated breast cancer or melanoma cells and among breast cancer and melanoma cells. Statistical analysis was performed using ANOVA and Bonferroni's post-hoc test.

### **Immunofluorescence**

RBECs were cultured until confluence on collagen/fibronectin-coated filter inserts. Tumor cells (MDA-MB-231 or A2058) were fluorescently labeled using Cell Tracker red (Life Technologies) and plated onto the endothelial monolayer. After 5 h cells were washed and fixed with ethanol/acetic acid. After blocking with 3% BSA, coverslips were incubated with anti-claudin-5 primary antibody (Life Technologies). The staining was visualized using a Alexa488-conjugated secondary antibody. Nuclei were stained with Hoechst 33342. Samples were mounted in FluoroMount-G (SouthernBiotech) and studied with a Nikon Eclipse TE2000U microscope connected to a digital camera (Spot RT KE, Diagnostic Instruments).

### **Cell viability assay**

Viability of tumor cells and endothelial cells was quantified with the EZ4U non-radioactive cell proliferation and cytotoxicity assay (Biomedica). D3, MDA-MB-231 and MCF-7 cells were seeded in 96-well plates. Next day the cells were treated for 5 h with 20  $\mu$ M EHT1864 or 25  $\mu$ M LY294002 in serum-free, phenol-red free DMEM. After incubation with EZ4U substrate for 45



min, the absorbance (OD at 450 nm) was detected using a BMG FLUOstar OPTIMA microplate reader.

### **Wound healing assay**

Tumor cells (MDA-MB-231, MCF-7 or A2058) were seeded into 24-well plates. After attachment the cell layer was wounded by scratching with a pipette tip, washed with PBS, and exposed to treatments with 20  $\mu$ M EHT1864 or 25  $\mu$ M LY294002 in serum-free Leibovitz's L-15 medium. Cells were monitored over 24 h, and phase contrast images were taken every 30 min with an Andor NEO sCMOS camera connected to the Nikon Eclipse Ti-E inverted microscope equipped with a home-built incubator set to 37°C and a 20 $\times$  Nikon Plan Fluor objective, all placed onto a Prior Proscan II motorized stage (Prior Scientific Instruments). The wound healing effect was quantified by averaging the number of migrating cells counted in five wounded areas.

### **Real-time impedance monitoring**

To monitor the effects of EHT1864 and LY294002 on D3 cells in real-time, we measured the electrical impedance using the xCELLigence system following the manufacturer's instructions (Acea Biosciences Inc.). Briefly, cells were seeded at a density of  $10^4$  cells/well into 100  $\mu$ l of media in an E-Plate® (i.e., 96-well tissue culture plates having micro-electrodes integrated on the bottom) and allowed to attach onto the electrode surface over time. The electrical impedance was recorded every 15 min. When the impedance reached plateau (i.e. confluent monolayer with

well-formed junctions), the cells were treated with 20  $\mu$ M EHT1864 or 25  $\mu$ M LY294002 for an additional 10 h. The cell impedance (which depends on cell number, degree of adhesion, spreading and proliferation of the cells and also the tightness of the junctions), expressed in arbitrary units (cell index) was automatically calculated by the software of the instrument.

### **Western-blot analysis**

Confluent D3 brain endothelial cells were treated with 20  $\mu$ M EHT1864 or 25  $\mu$ M LY294002 for 5 h. Cells were washed with PBS and scraped into ice-cold RIPA buffer (20 mM Tris, 150 mM NaCl, 0.5% Triton X-100, 1% sodium deoxycholate, 0.1% sodium dodecyl sulphate, 1 mM sodium vanadate, 10 mM NaF, 1 mM EDTA, 1 mM Pefabloc) and incubated on ice for 30 min. Lysates were clarified by centrifugation at 10,000 g for 10 min at 4°C. Proteins were electrophoresed and blotted onto nitrocellulose (Bio-Rad) membranes. Blocking was carried out at room temperature for 30 min in TBS-T containing 3% BSA. Anti-claudin-5 (Invitrogen), primary antibody was used. After washing the membranes in TBS-T, blots were incubated with the HRP-conjugated secondary antibody diluted in TBS-T. The immunoreaction was visualized using Clarity ECL Western Blot Substrate kit (Bio-Rad) in a Bio-Rad ChemiDoc MP Imaging System.

### **ACKNOWLEDGEMENTS**

This work was supported by grants from the Hungarian Scientific Research Fund (OTKA PD-100958, K-100807, K-116158, PD-115697, PD-112509), the National Development Agency

(Hungary-Romania Cross-Border Co-operation Programme 2007-2013: HURO/1101/173/2.2.1) and the “Lendület” Program of the Hungarian Academy of Sciences. A.G.V. and I.W. are recipients of the János Bolyai Research Fellowship of the Hungarian Academy of Sciences (BO/00598/14/8 and BO/00320/12/8).

Accepted Manuscript

## REFERENCES

1. Lorger M, Felding-Habermann B. Capturing changes in the brain microenvironment during initial steps of breast cancer brain metastasis. *Am J Pathol* 2010; 176:2958-71.
2. Wilhelm I, Molnar J, Fazakas C, Hasko J, Krizbai IA. Role of the blood-brain barrier in the formation of brain metastases. *International journal of molecular sciences* 2013; 14:1383.
3. Valiente M, Obenauf AC, Jin X, Chen Q, Zhang XH, Lee DJ, et al. Serpins promote cancer cell survival and vascular co-option in brain metastasis. *Cell* 2014; 156:1002-16.
4. Bugyik E, Dezso K, Reiniger L, László V, Tóvári J, Tímár J, et al. Lack of angiogenesis in experimental brain metastases. *J Neuropathol Exp Neurol* 2011; 70:979-91.
5. Kim SW, Choi HJ, Lee HJ, He J, Wu Q, Langley RR, et al. Role of the endothelin axis in astrocyte- and endothelial cell-mediated chemoprotection of cancer cells. *Neuro Oncol* 2014; 16:1585-98.
6. Hamilla SM, Stroka KM, Aranda-Espinoza H. VE-cadherin-independent cancer cell incorporation into the vascular endothelium precedes transmigration. *PLoS One* 2014; 9:e109748.
7. Wilhelm I, Krizbai IA. In vitro models of the blood-brain barrier for the study of drug delivery to the brain. *Mol Pharm* 2014; 11:1949-63.

8. Fazakas C, Wilhelm I, Nagyoszi P, Farkas AE, Hasko J, Molnar J, et al. Transmigration of melanoma cells through the blood-brain barrier: role of endothelial tight junctions and melanoma-released serine proteases. *PloS one* 2011; 6:e20758.
9. Khuon S, Liang L, Dettman RW, Sporn PH, Wysolmerski RB, Chew TL. Myosin light chain kinase mediates transcellular intravasation of breast cancer cells through the underlying endothelial cells: a three-dimensional FRET study. *J Cell Sci* 2010; 123:431-40.
10. Arvanitis C, Khuon S, Spann R, Ridge KM, Chew TL. Structure and biomechanics of the endothelial transcellular circumferential invasion array in tumor invasion. *PLoS One* 2014; 9:e89758.
11. Wilhelm I, Fazakas C, Molnar J, Hasko J, Vegh AG, Cervenak L, et al. Role of Rho/ROCK signaling in the interaction of melanoma cells with the blood-brain barrier. *Pigment cell & melanoma research* 2014; 27:113.
12. Parri M, Chiarugi P. Rac and Rho GTPases in cancer cell motility control. *Cell communication and signaling : CCS* 2010; 8:23.
13. Symons M, Segall JE. Rac and Rho driving tumor invasion: who's at the wheel? *Genome biology* 2009; 10:213.
14. Wertheimer E, Gutierrez-Uzquiza A, Rosemlit C, Lopez-Haber C, Sosa MS, Kazanietz MG. Rac signaling in breast cancer: a tale of GEFs and GAPs. *Cell Signal* 2012; 24:353-62.

15. Ebi H, Costa C, Faber AC, Nishtala M, Kotani H, Juric D, et al. PI3K regulates MEK/ERK signaling in breast cancer via the Rac-GEF, P-Rex1. *Proc Natl Acad Sci U S A* 2013; 110:21124-9.
16. Akinleye A, Avvaru P, Furqan M, Song Y, Liu D. Phosphatidylinositol 3-kinase (PI3K) inhibitors as cancer therapeutics. *J Hematol Oncol* 2013; 6:88.
17. Liu P, Cheng H, Roberts TM, Zhao JJ. Targeting the phosphoinositide 3-kinase pathway in cancer. *Nat Rev Drug Discov* 2009; 8:627-44.
18. Schlegel NC, von Planta A, Widmer DS, Dummer R, Christofori G. PI3K signalling is required for a TGF $\beta$ -induced epithelial-mesenchymal-like transition (EMT-like) in human melanoma cells. *Exp Dermatol* 2015; 24:22-8.
19. Sadeghi N, Gerber DE. Targeting the PI3K pathway for cancer therapy. *Future Med Chem* 2012; 4:1153-69.
20. Welf ES, Ahmed S, Johnson HE, Melvin AT, Haugh JM. Migrating fibroblasts reorient directionality by a metastable, PI3K-dependent mechanism. *J Cell Biol* 2012; 197:105-14.
21. Fidler IJ, Schackert G, Zhang RD, Radinsky R, Fujimaki T. The biology of melanoma brain metastasis. *Cancer metastasis reviews* 1999; 18:387.
22. Denkins Y, Reiland J, Roy M, Sinnappah-Kang ND, Galjour J, Murry BP, et al. Brain metastases in melanoma: roles of neurotrophins. *Neuro Oncol* 2004; 6:154-65.

23. Rozenberg GI, Monahan KB, Torrice C, Bear JE, Sharpless NE. Metastasis in an orthotopic murine model of melanoma is independent of RAS/RAF mutation. *Melanoma Res* 2010; 20:361-71.
24. Boussemart L, Malka-Mahieu H, Girault I, Allard D, Hemmingsson O, Tomasic G, et al. eIF4F is a nexus of resistance to anti-BRAF and anti-MEK cancer therapies. *Nature* 2014; 513:105-9.
25. Safuan S, Storr SJ, Patel PM, Martin SG. A comparative study of adhesion of melanoma and breast cancer cells to blood and lymphatic endothelium. *Lymphat Res Biol* 2012; 10:173-81.
26. Davies MA, Stemke-Hale K, Lin E, Tellez C, Deng W, Gopal YN, et al. Integrated Molecular and Clinical Analysis of AKT Activation in Metastatic Melanoma. *Clinical cancer research : an official journal of the American Association for Cancer Research* 2009; 15:7538.
27. Xing F, Persaud Y, Pratilas CA, Taylor BS, Janakiraman M, She QB, et al. Concurrent loss of the PTEN and RB1 tumor suppressors attenuates RAF dependence in melanomas harboring (V600E)BRAF. *Oncogene* 2012; 31:446-57.
28. Peng HH, Hodgson L, Henderson AJ, Dong C. Involvement of phospholipase C signaling in melanoma cell-induced endothelial junction disassembly. *Front Biosci* 2005; 10:1597-606.
29. Niessner H, Forscher A, Klumpp B, Honegger JB, Witte M, Bornemann A, et al. Targeting hyperactivation of the AKT survival pathway to overcome therapy resistance of melanoma brain metastases. *Cancer Med* 2013; 2:76-85.

30. Li B, Zhao WD, Tan ZM, Fang WG, Zhu L, Chen YH. Involvement of Rho/ROCK signalling in small cell lung cancer migration through human brain microvascular endothelial cells. *FEBS Lett* 2006; 580:4252-60.
31. Mierke CT. Cancer cells regulate biomechanical properties of human microvascular endothelial cells. *J Biol Chem* 2011; 286:40025-37.
32. Campa CC, Ciralo E, Ghigo A, Germina G, Hirsch E. Crossroads of PI3K and Rac pathways. *Small GTPases* 2015; 6:71-80.
33. Rodon J, Dienstmann R, Serra V, Tabernero J. Development of PI3K inhibitors: lessons learned from early clinical trials. *Nat Rev Clin Oncol* 2013; 10:143-53.
34. Wilhelm I, Farkas AE, Nagyoszi P, Váró G, Bálint Z, Végh GA, et al. Regulation of cerebral endothelial cell morphology by extracellular calcium. *Phys Med Biol* 2007; 52:6261-74.
35. Qin D, Xia Y, Whitesides GM. Soft lithography for micro- and nanoscale patterning. *Nat Protoc* 2010; 5:491-502.
36. Song JW, Gu W, Futai N, Warner KA, Nor JE, Takayama S. Computer-controlled microcirculatory support system for endothelial cell culture and shearing. *Anal Chem* 2005; 77:3993-9.



**Table 1. Comparison of the adhesion of MDA-MB-231, MCF-7, A2058 and A375 cells to D3 brain endothelial monolayers.** % of plated cells is represented (mean and SD); p value was assessed using ANOVA and Bonferroni's post-hoc test.

<b>Table 1</b>				
	D3+MDA-MB-231	D3+MCF-7	D3+A2058	D3+A375
average	18.44%	18.15%	34.64%	35.05%
st dev	8.66%	8.92%	7.41%	0.75%
p	<0.05 vs. A2058 or A375	<0.05 vs. A2058 or A375	<0.05 vs. MDA or MCF	<0.05 vs. MDA or MCF

**Table 2. Comparison of transmigration of MDA-MB-231, A2058 and A375 cells through D3 brain endothelial monolayers under static conditions.** % of plated cells is represented (mean and SD); p value was assessed using Student's test.

<b>Table 2</b>			
	D3+MDA-MB-231	D3+A2058	D3+A375
average	15.78%	26.99%	28.28%
st dev	0.82%	2.54%	4.72%
p	<0.05 vs. A2058 or A375	<0.05 vs. MDA-MB-231	<0.05 vs. MDA-MB-231

**Table 3. Comparison of transmigration of A2058 and MDA-MB-231 cells through D3 brain endothelial monolayers under dynamic conditions.** MDA-MB-231 breast cancer cells or A2058 melanoma cells were injected into the microchannels already containing confluent D3 monolayers. Tumor cells were monitored for 6 h under a continuous medium flow of 100  $\mu$ l/h. Tumor cells were divided into four groups: cells washed away by the flow of the culture medium (no attachment), cells not transmigrating in 6 h (no transmigration), cells migrating through the brain endothelium in the first 20 min (transmigr. in 20 min) and cells transmigrating after 20 min (transmigr. in >20 min). % of plated cells is represented (mean and SD); p value (comparing D3+MDA-MB-231 and D3+A2058) was assessed with ANOVA and Bonferroni's post-hoc test.

<b>Table 3</b>				
	D3+MDA-MB-231			
	no attachment	no transmigration	transmigr. in 20 min	transmigr. in >20 min
average	50.00%	<b>15.00%</b>	<b>2.80%</b>	32.20%
st dev	4.24%	4.04%	1.73%	3.54%
	D3+A2058			
	no attachment	no transmigration	transmigr. in 20 min	transmigr. in >20 min
average	42.50%	<b>4.50%</b>	<b>23.50%</b>	29.50%
st dev	7.21%	1.00%	4.95%	5.12%
p		<0.05	<0.05	

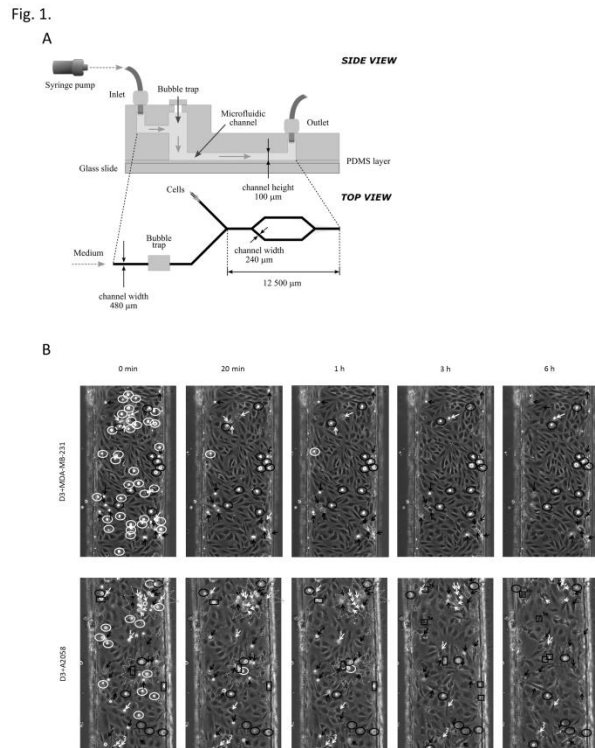


**Fig. 1. Dynamic transmigration experimental setup.** **A:** Schematic representation of the microfluidic device. **B:** Images used for constructing the time lapse videos (presented in Suppl. videos 2 and 3). D3 cells were cultured until confluence in the microfluidic device, then tumor cells were injected and left under a continuous flow of 100  $\mu\text{l/h}$  for 6 h. Phase contrast images were taken every 5 min. Individual tumor cells were marked as follows: white circle = no attachment, black circle = no transmigration, white arrow = transmigration in 20 min, black arrow = transmigration in >20 min, black box = division. The grey dotted stars delineate clusters of transmigrating melanoma cells.

Fig. 2.

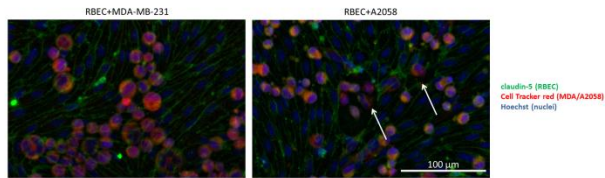


**Fig. 2. Effect of breast cancer and melanoma cells on the tight junctions of brain endothelial cells.** MDA-MB-231 breast cancer cells or A2058 melanoma cells labeled in red were plated onto confluent RBEC monolayers and left for 5 h. Tight junctions of endothelial cells were stained in green using anti-claudin-5 antibodies. Arrows indicate disappearance of claudin-5 staining.

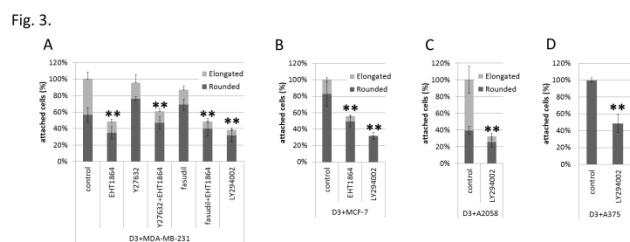


**Fig. 3. Effect of Rac- or PI3K-inhibition on the adhesion of breast cancer cells or melanoma cells onto the brain endothelium.** Fluorescently labeled MDA-MB-231 (A), MCF-7 breast cancer cells (B), A2058 (C) or A375 melanoma cells (D) were plated onto confluent D3 monolayers and left for 90 min. After washing of non-adherent cells, attached tumor cells were counted. Results are expressed as % control and given as mean  $\pm$  SD. N = 3, \*\* = P<0.01, as assessed by ANOVA and Bonferroni's post-hoc test.

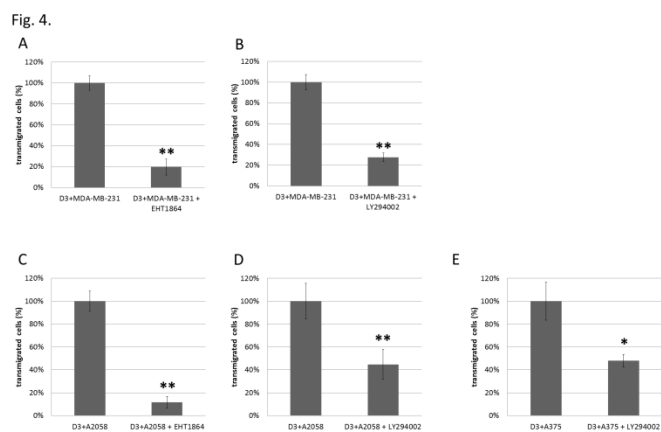


**Fig. 4. Effect of Rac- or PI3K-inhibition on the transmigration of breast cancer cells or melanoma cells through the brain endothelium in static conditions.** MDA-MB-231 breast cancer cells (**A, B**), A2058 (**C, D**) or A375 melanoma cells (**E**) were plated onto confluent D3 monolayers and left for 6 h. Phase-contrast images were made every 5 min and transmigrating tumor cells were counted. Results are expressed as % control and given as mean  $\pm$  SD. N = 3, \*\* =  $P < 0.01$ , \* =  $P < 0.05$  as assessed by Student's t-test.

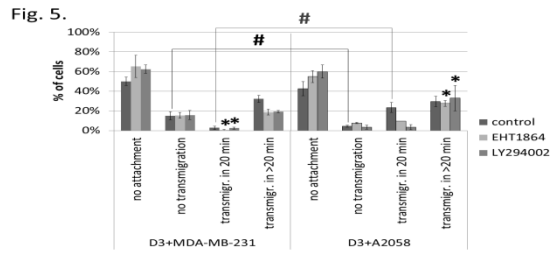


**Fig. 5. Effect of Rac- or PI3K-inhibition on the transmigration of breast cancer cells or melanoma cells through the brain endothelium in dynamic conditions.** Results are expressed as % control and given as mean  $\pm$  SD. N = 3, \* =  $P < 0.05$  EHT1864- or LY294002-treated cells compared to control, # =  $P < 0.05$  A2058 cells compared to MDA-MB-231 cells, as assessed by ANOVA and Bonferroni's post-hoc test.



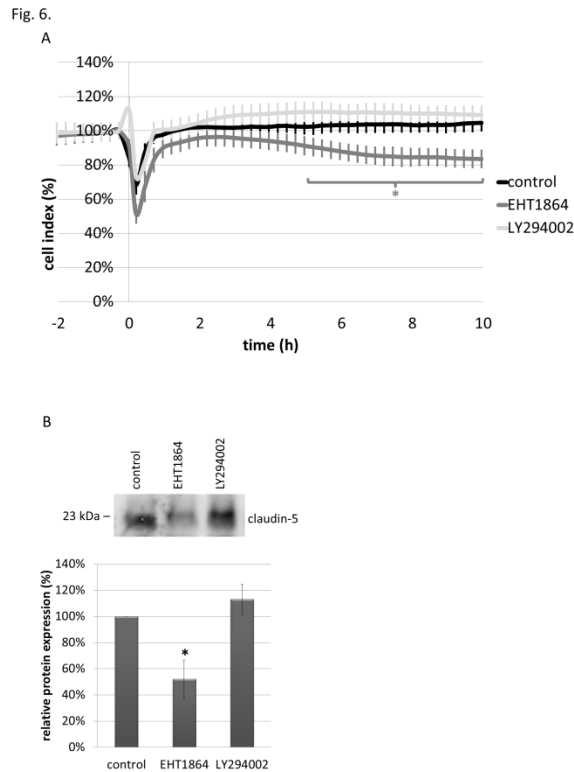


**Fig. 6. Effect of the Rac inhibitor EHT1864 on the junctional integrity of the brain endothelium. A:** The impedance of D3 brain endothelial cells (represented by the cell index) was assessed by the ACEA xCELLigence system. Results are expressed as % control and given as mean  $\pm$  SD. N = 3, \* =  $P < 0.05$  compared to control, as assessed by ANOVA and Bonferroni's post-hoc test. **B:** D3 cells were treated with 20  $\mu$ M EHT1864 or 25  $\mu$ M LY294002 for 5 h. Claudin-5 western-blot was performed from the RIPA-soluble fraction. One representative blot and densitometry based on three independent experiments is shown. \* =  $P < 0.05$  compared to control, as assessed by ANOVA and Bonferroni's post-hoc test.